Supplementary Information

Octahedral Copper(II)-diimine Complexes of Triethylenetetramine: Effect of Stereochemical Fluxionality and Ligand Hydrophobicity on Cu^{II}/Cu^{I} Redox, DNA Binding and Cleavage, Cytotoxicity and Apoptosis-inducing Ability

Mitu Sharma,[a] Mani Ganeshpandian,[b] Munmi Majumder,[c] Ajaykamal Tamilarasan,[d] Mukesh Sharma,[a] Rupak Mukhopadhyay,[c] Nashreen S. Islam[a]* and Mallayan Palaniandavar[d]*

[a]*Department of Chemical Sciences, Tezpur University, Tezpur 784 028, India*
[b]*Department of Chemistry, SRM Institute of Science & Technology, Kattankulathur, Chennai 603 203, Tamil Nadu, India.*
[c]*Department of Molecular Biology and Biotechnology, Tezpur University, Tezpur 784 028, India*
[d]*School of Chemistry, Bharathidasan University, Tiruchirappalli 620 024, Tamil Nadu, India*

Synthesis of $[Cu(dien)(bpy)](ClO_4)_2$ and $[Cu(dien)(phen)](ClO_4)_2$

A methanol:acetonitrile solution (5:1v/v) of copper(II) perchlorate hexahydrate (0.37 g, 1 mmol) was added dropwise with stirring to a methanolic solution of diethylenetriamine (0.13 g, 1 mmol). A methanolic solution of 2,2'-bipyridine (0.156 g, 1 mmol) / 1,10-phenanthroline (0.198 g, 1mmol) was added to this mixture and stirred for 1 h at room temperature. The resulting solution was kept aside for 24h. Dark blue crystals of $[Cu(dien)(bpy)](ClO_4)_2$ and a blue precipitate of complex $[Cu(dien)(phen)](ClO_4)_2$ were obtained. The latter was recrystallized to obtain crystalline product.

Experimental Methods

DNA Binding Experiment

For all the experiments, concentrated stock solutions of metal complexes were prepared with CH_3CN solvent followed by dilution with 5 mM Tris-HCl/50mM NaCl buffer at pH 7.2 to prepare required concentration of solution. Prior to the absorption spectral titrations, the DNA solutions were pretreated with the solutions of metal complexes to ensure that no change in the concentration of the metal complexes occur during titration. Hence the spectral changes do not occur by dilution factor. Absorption spectral titration experiments were carried out by maintaining a constant concentration of the complex and varying the nucleic acid concentration. To achieve this, an appropriate amount of the metal complex was dissolved in tris buffer solution and mixed with DNA stock solutions, while maintaining the total volume constant (1 ml). This resulted in a series of solutions with varying concentrations of DNA but with a constant concentration of the complex. The solutions were thoroughly mixed using a micropipette and allowed to equilibrate for 10 min prior to measurements wherever required. DNA was also added to the reference cuvette to correct for any absorbance or light scattering due to DNA itself. The absorbance of solutions of the complexes was recorded after successive addition of CT DNA.

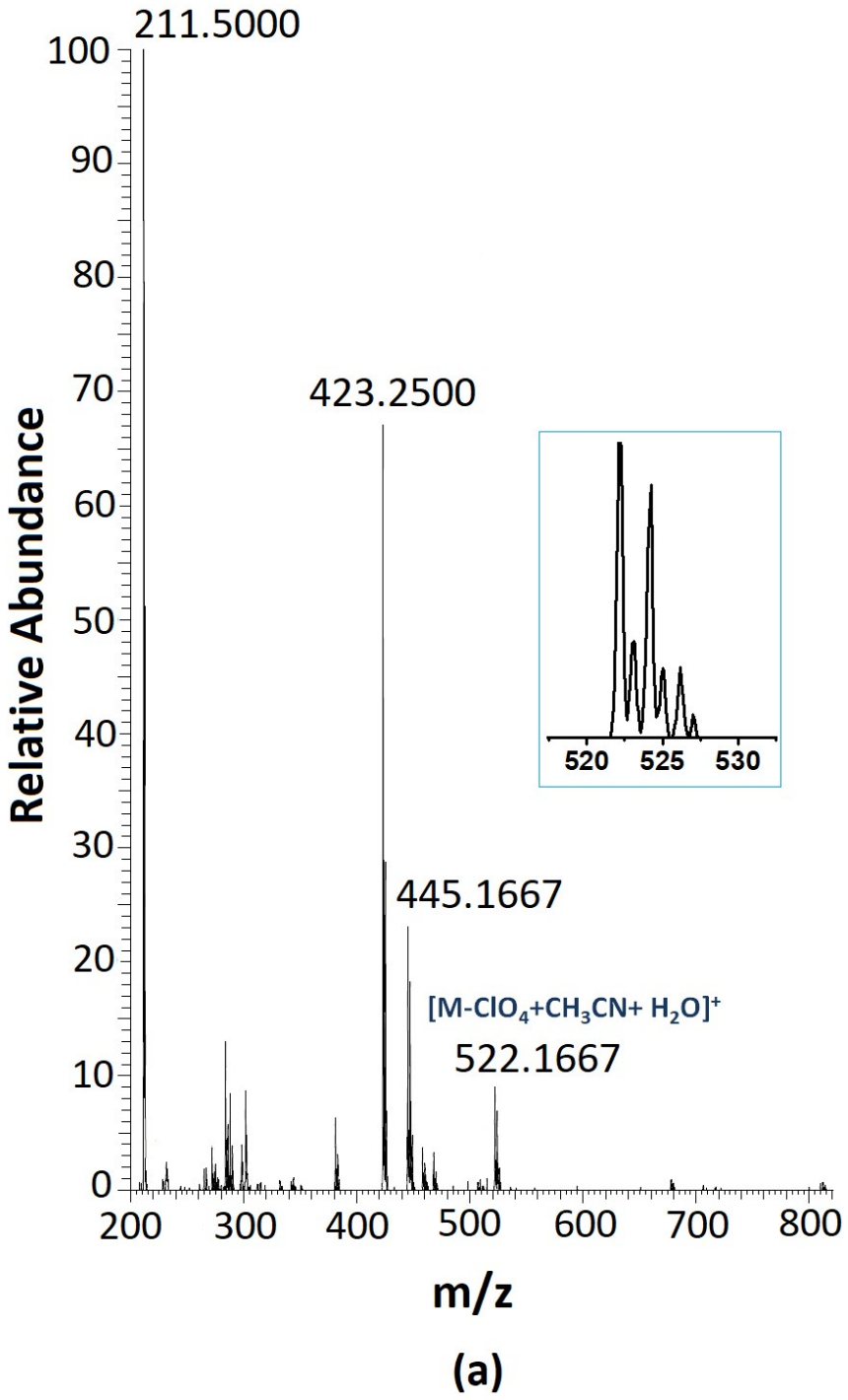

Fig. S1(a) HR-MS of $[Cu(trien)(bpy)](ClO_4)_2$ **1** in CH_3CN solution. Inset: Isotropic distributions for the parent (m/z = 522.1667) peak.

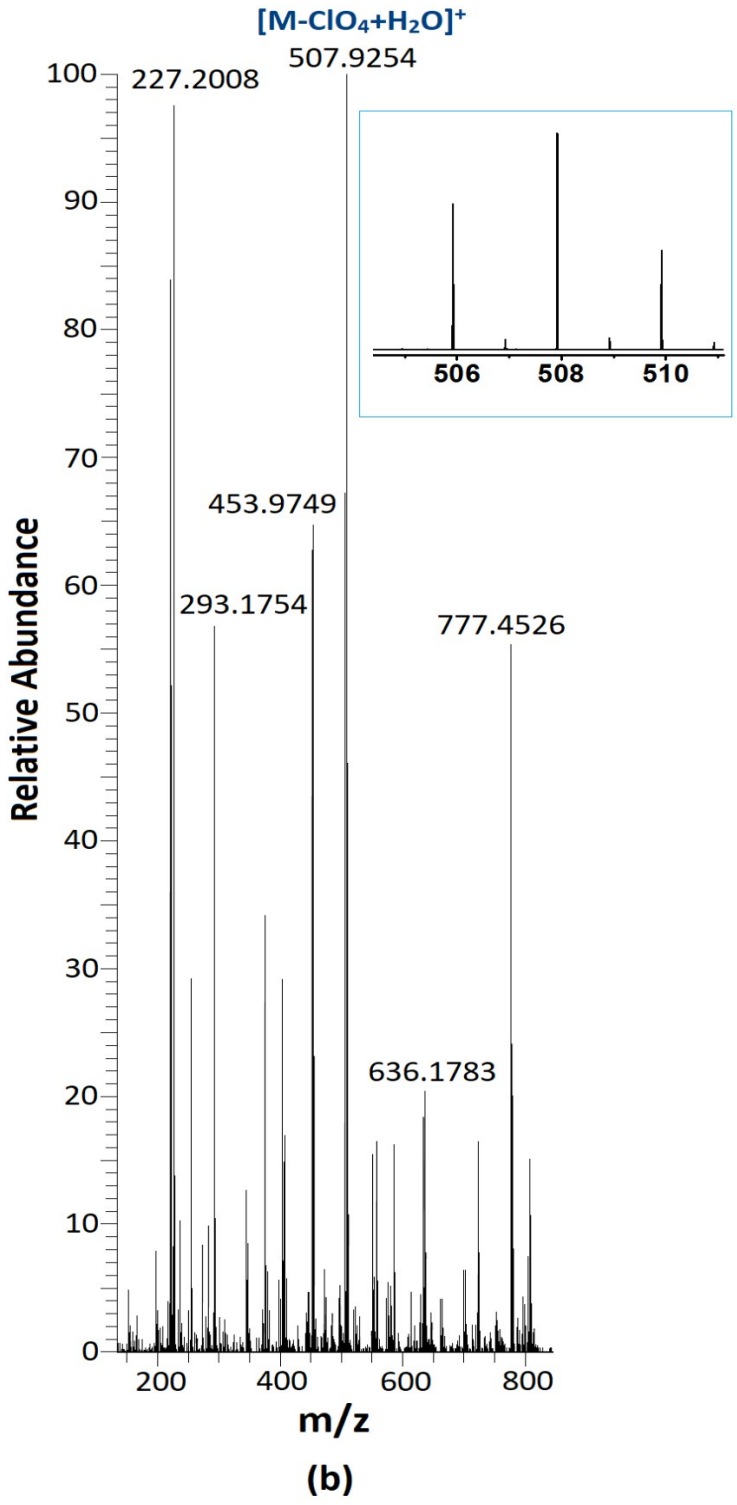

Fig. S1(b) HR-MS of [Cu(trien)(phen)]$(ClO_4)_2$ **2** in CH_3CN solution. Inset: Isotropic distributions for the parent (m/z = 507.9254) peak.

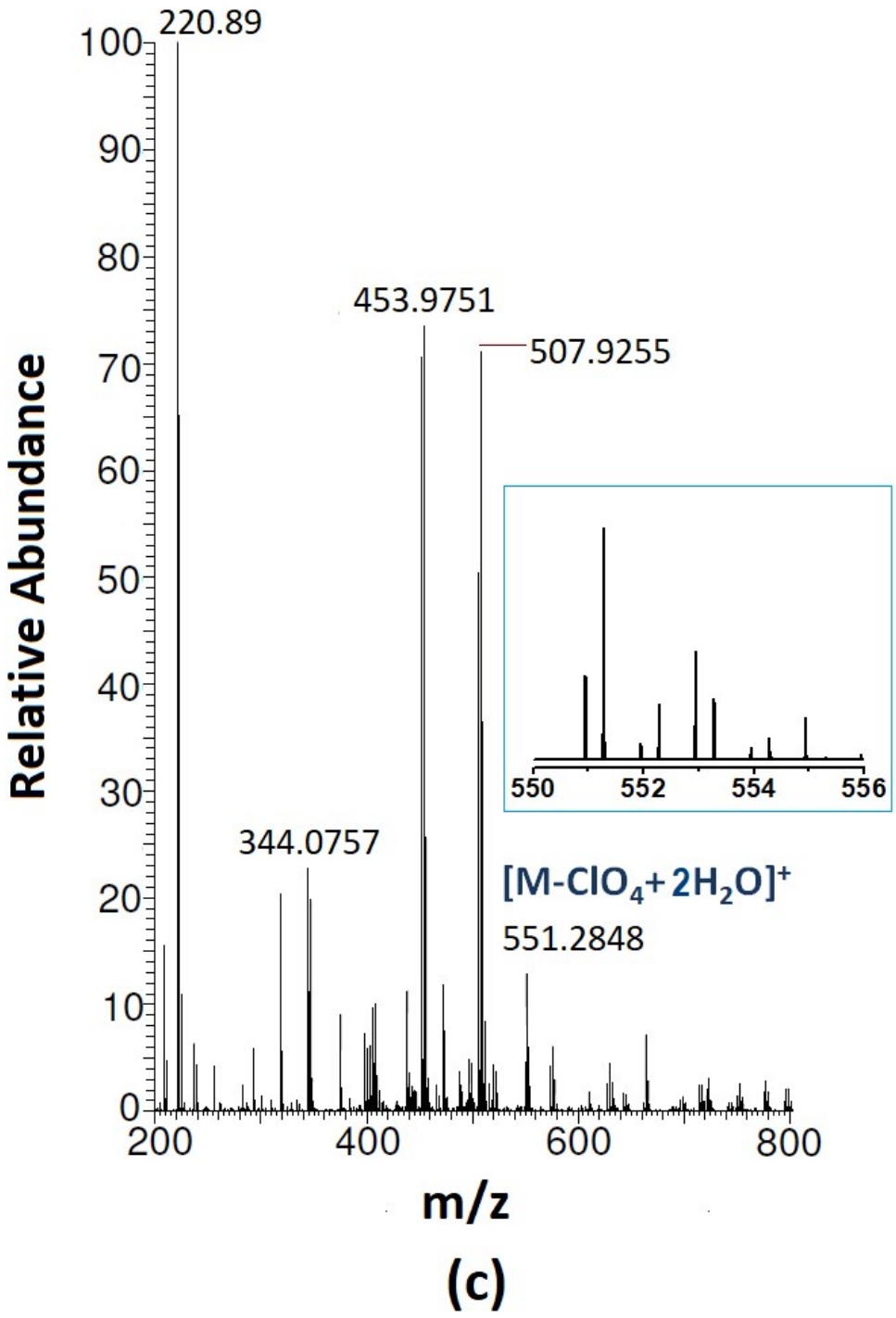

Fig. S1(c) HR-MS of [Cu(trien)(5,6-dmp)]$(ClO_4)_2$ **3** in CH_3CN solution. Inset: Isotropic distributions for the parent (m/z = 551.2848) peak.

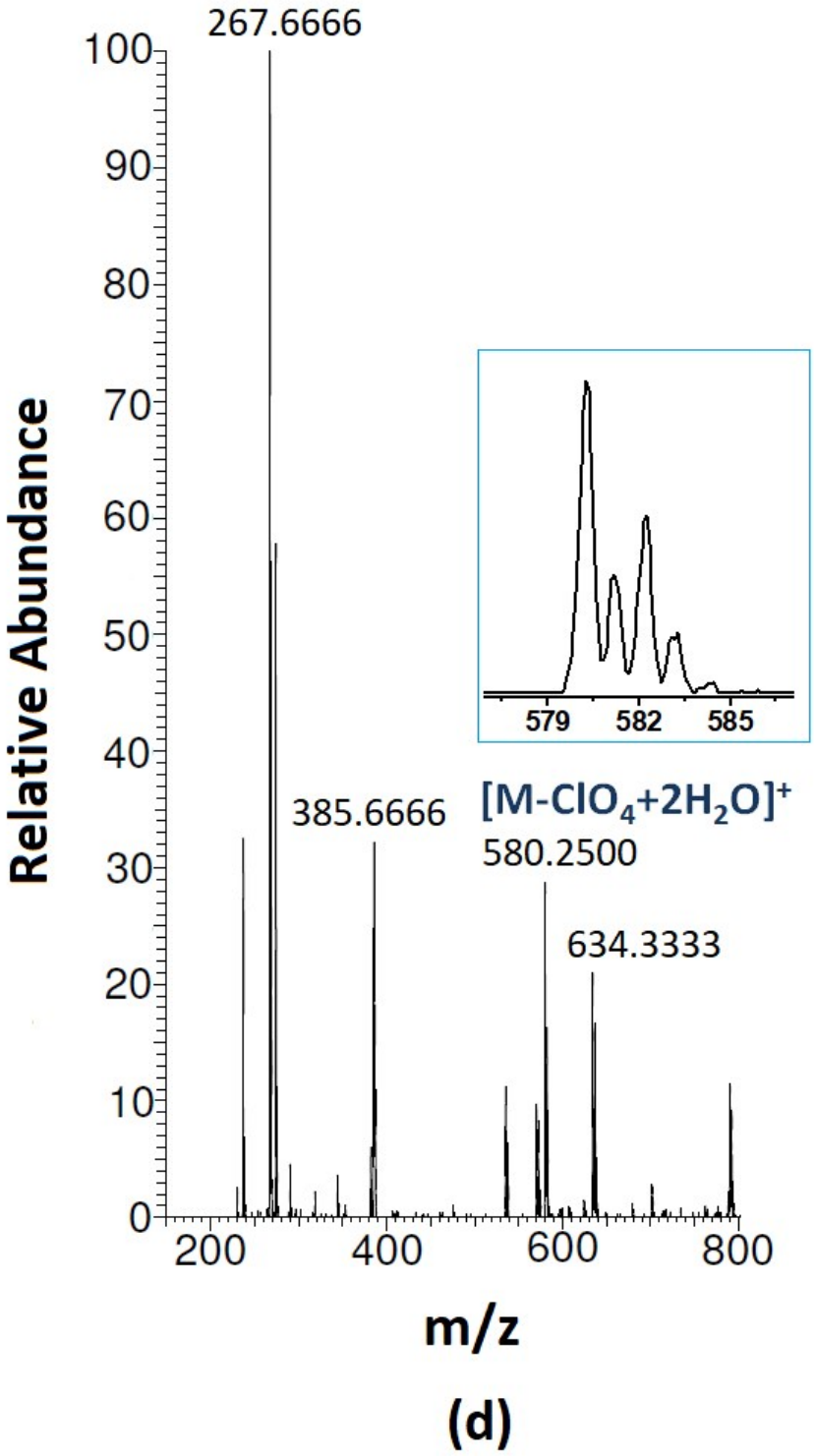

Fig. S1(d) HR-MS of [Cu(trien)(3,4,7,8-tmp)]$(ClO_4)_2$ **4** in CH_3CN solution. Inset: Isotropic distributions for the parent (m/z = 580.2500) peak.

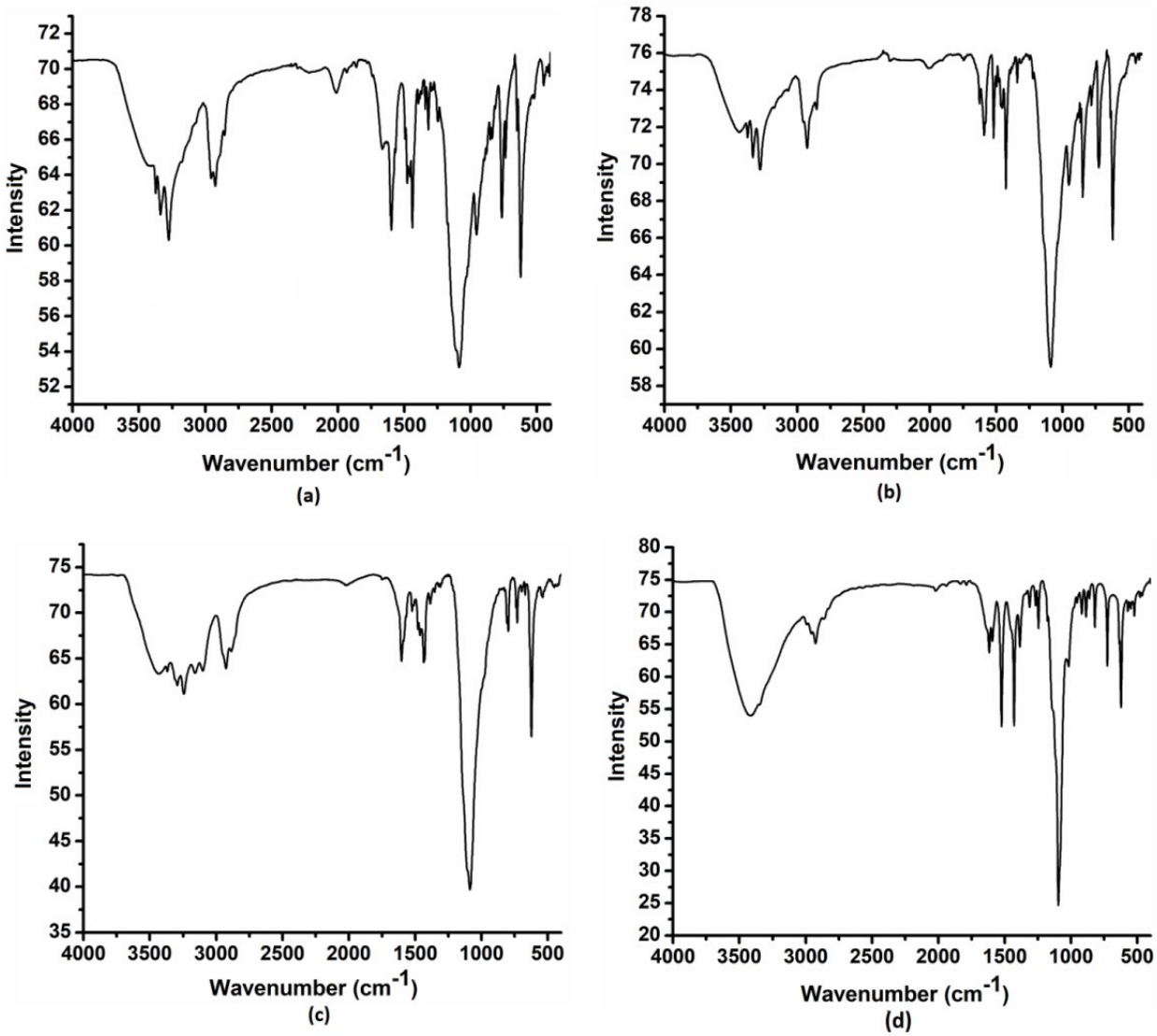

Fig. S2 IR spectrum of complex $[Cu(trien)(bpy)](ClO_4)_2$ **1** (a), $[Cu(trien)(phen)](ClO_4)_2$ **2** (b), $[Cu(trien)(5,6\text{-dmp})](ClO_4)_2$ **3** (c) and $[Cu(trien)(3,4,7,8\text{-tmp})](ClO_4)_2$ **4** (d).

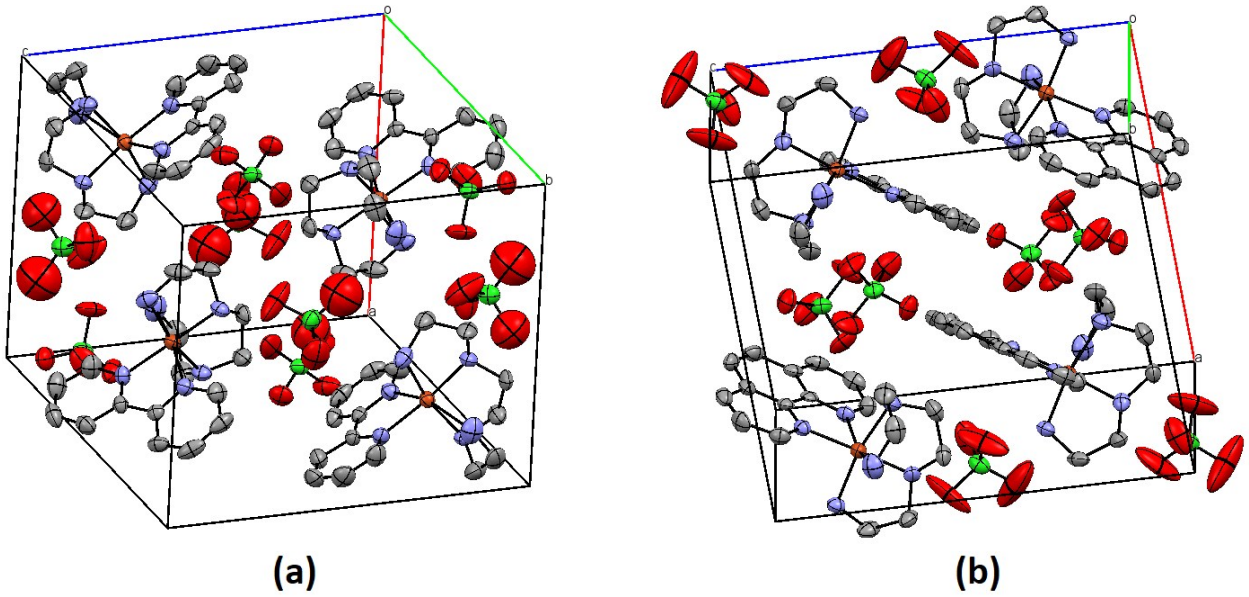

Fig. S3 The unit cell packing diagrams of complexes $[Cu(trien)(bpy)](ClO_4)_2$ **1** (a) and $[Cu(trien)(phen)](ClO_4)_2$ **2** (b).

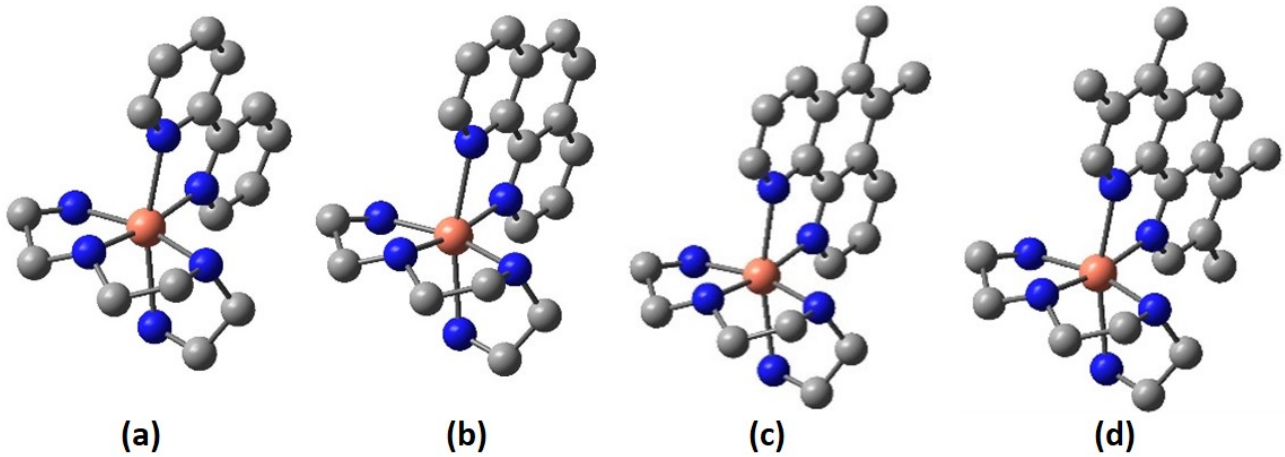

Fig. S4 Ball-and-stick representation of DFT Optimized structures of $[Cu(trien)(bpy)]^{2+}$ **1** (a), $[Cu(trien)(phen)]^{2+}$ **2** (b), $[Cu(trien)(5,6\text{-dmp})]^{2+}$ **3** (c) and $[Cu(trien)(3,4,7,8\text{-tmp})]^{2+}$ **4** (d). Colour scheme: blue, nitrogen; orange, copper; grey, carbon.

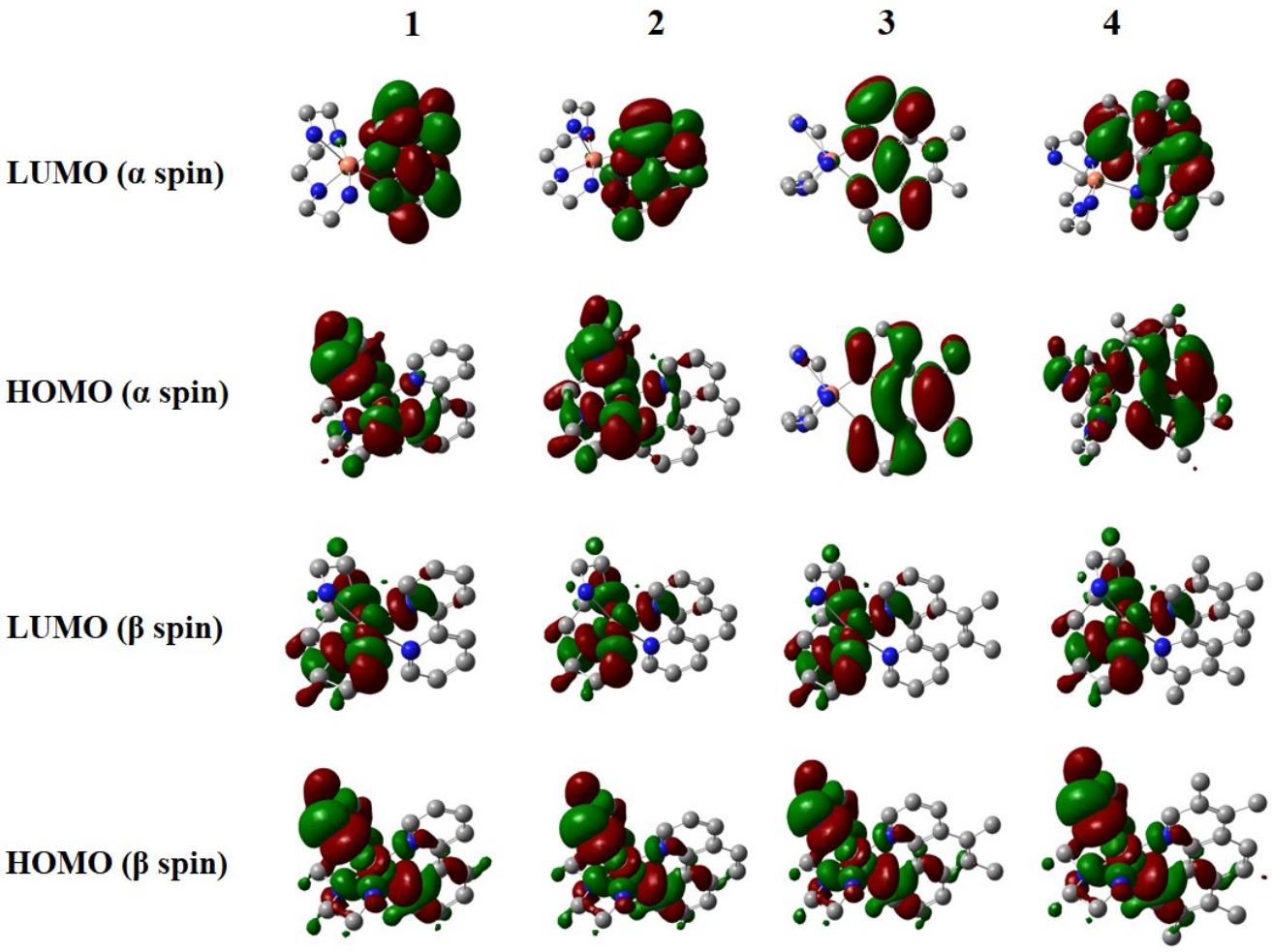

Fig. S5 Computed frontier molecular orbitals of complexes $[Cu(trien)(bpy)]^{2+}$ **1**, $[Cu(trien)(phen)]^{2+}$ **2**, $[Cu(trien)(5,6\text{-dmp})]^{2+}$ **3** and $[Cu(trien)(3,4,7,8\text{-tmp})]^{2+}$**4**, calculated at the B3LYP 6-31G/ LANL2DZ levels.

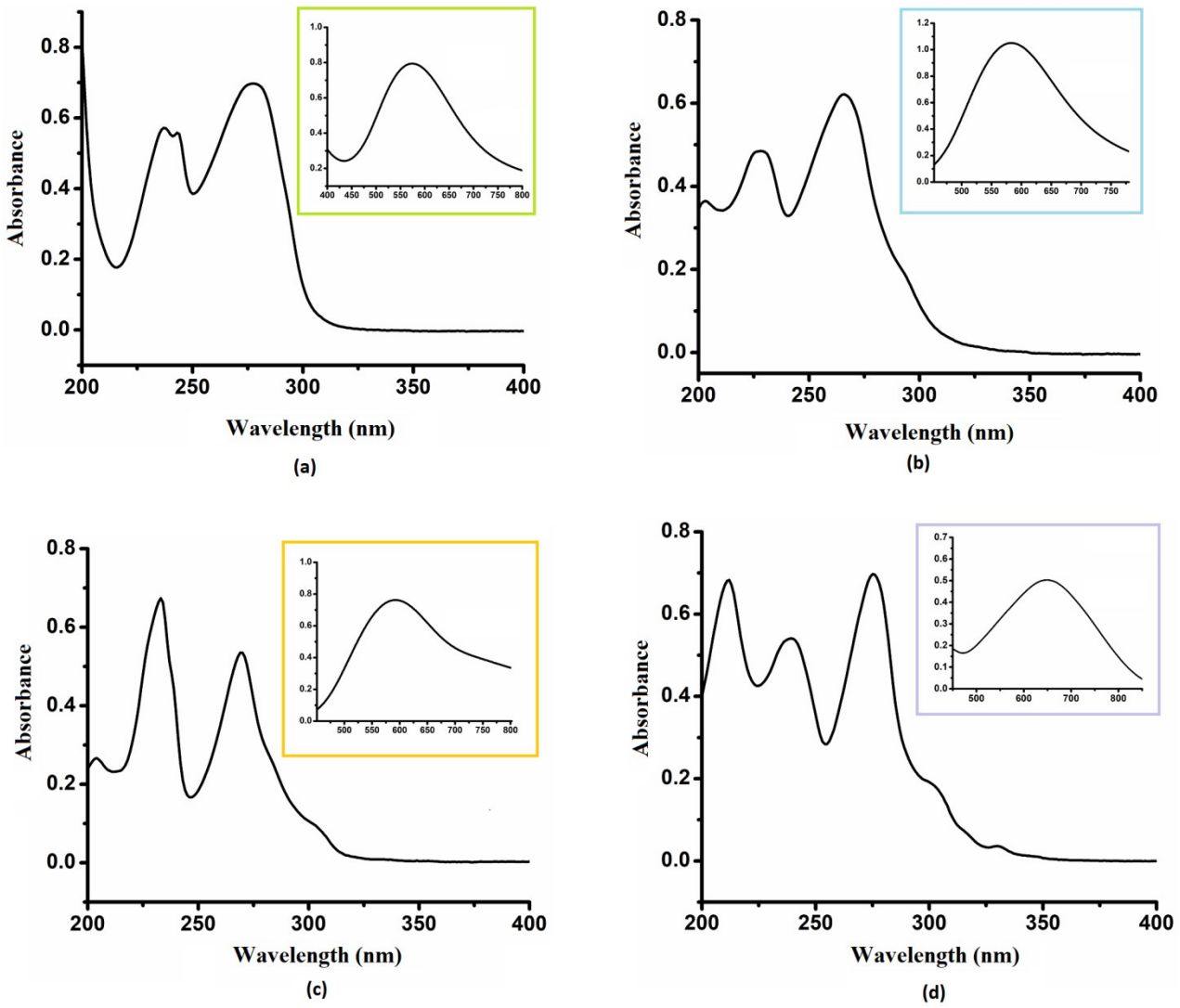

Fig. S6 UV-Vis absorption spectra of $[Cu(trien)(bpy)](ClO_4)_2$ **1** (a), $[Cu(trien)(phen)](ClO_4)_2$ **2** (b), $[Cu(trien)(5,6\text{-dmp})](ClO_4)_2$ **3** (c) and $[Cu(trien)(3,4,7,8\text{-tmp})](ClO_4)_2$ **4** (d) in CH_3CN solution (conc: 1.5×10^{-5} M; Inset conc: 5×10^{-3} M)

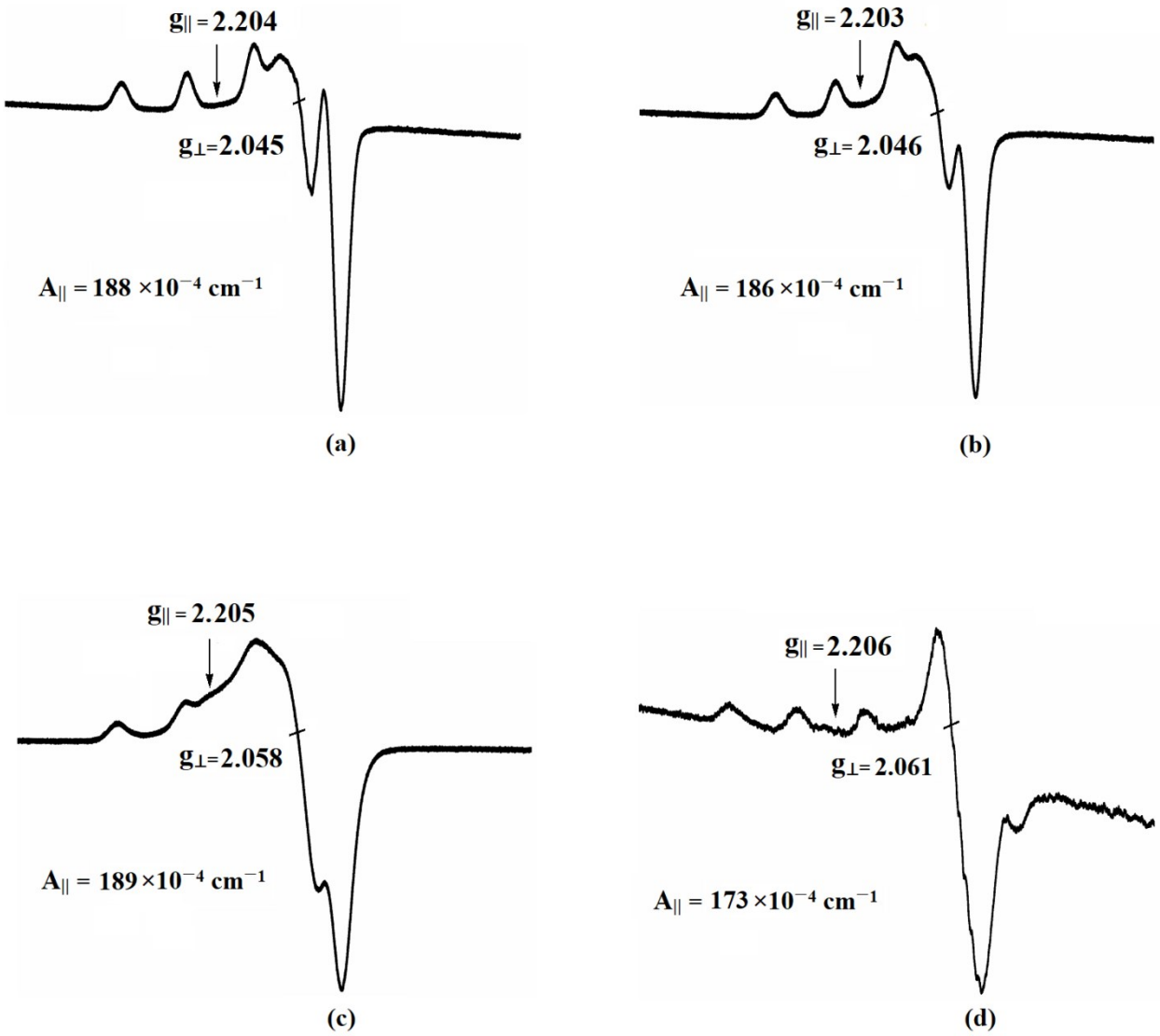

Fig. S7 Frozen solution EPR spectra of [Cu(trien)(bpy)]$(ClO_4)_2$ **1** (a), [Cu(trien)(phen)]$(ClO_4)_2$ **2** (b), [Cu(trien)(5,6-dmp)]$(ClO_4)_2$ **3** (c) and [Cu(trien)(3,4,7,8-tmp)]$(ClO_4)_2$ **4** (d) in CH_3CN : acetone (4:1 v/v) at LNT.

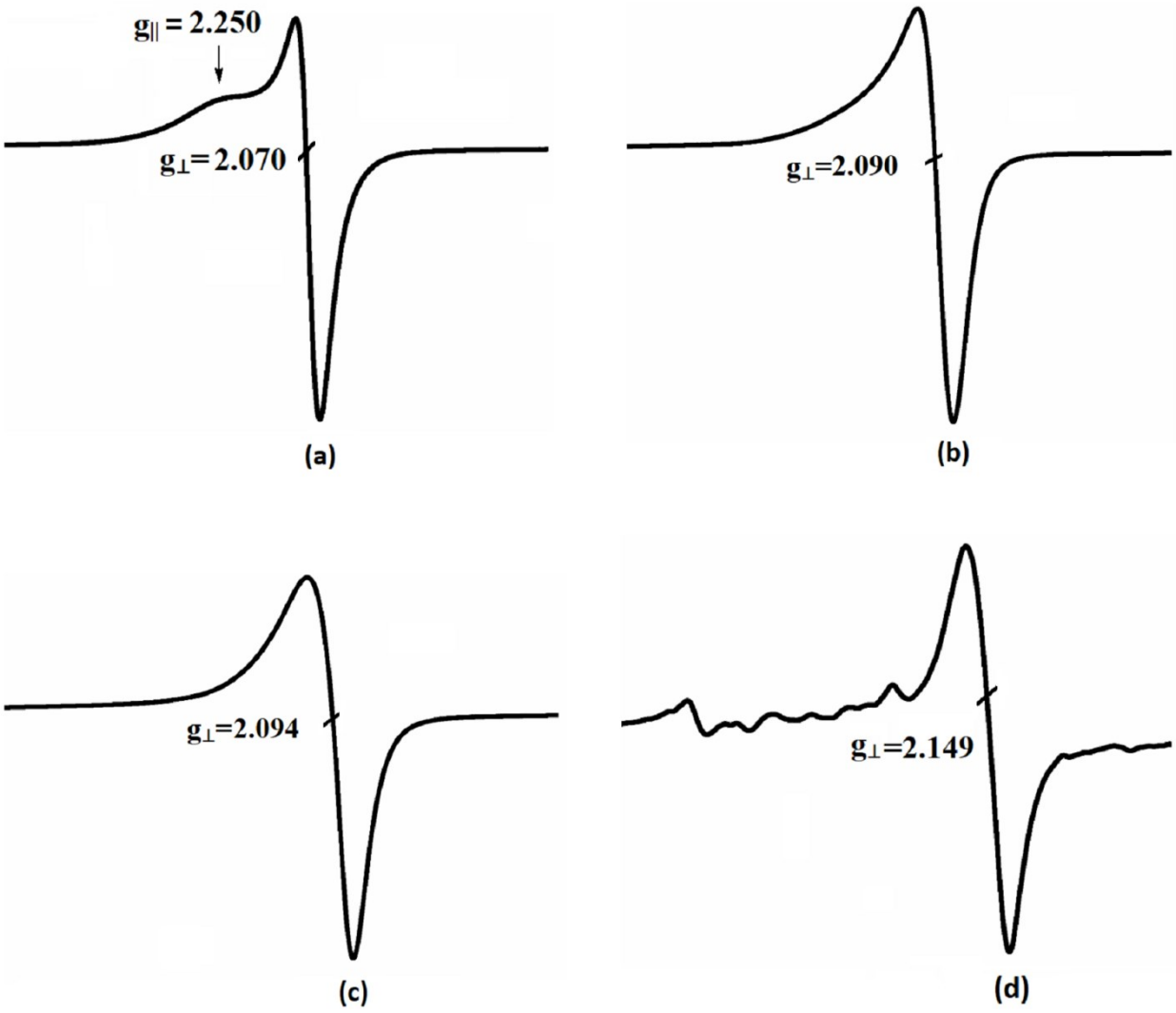

Fig. S8 Polycrystalline EPR spectra of [Cu(trien)(bpy)]$(ClO_4)_2$ **1** (a), [Cu(trien)(phen)]$(ClO_4)_2$ **2** (b), [Cu(trien)(5,6-dmp)]$(ClO_4)_2$ **3** (c) and [Cu(trien)(3,4,7,8-tmp)]$(ClO_4)_2$ **4** (d).

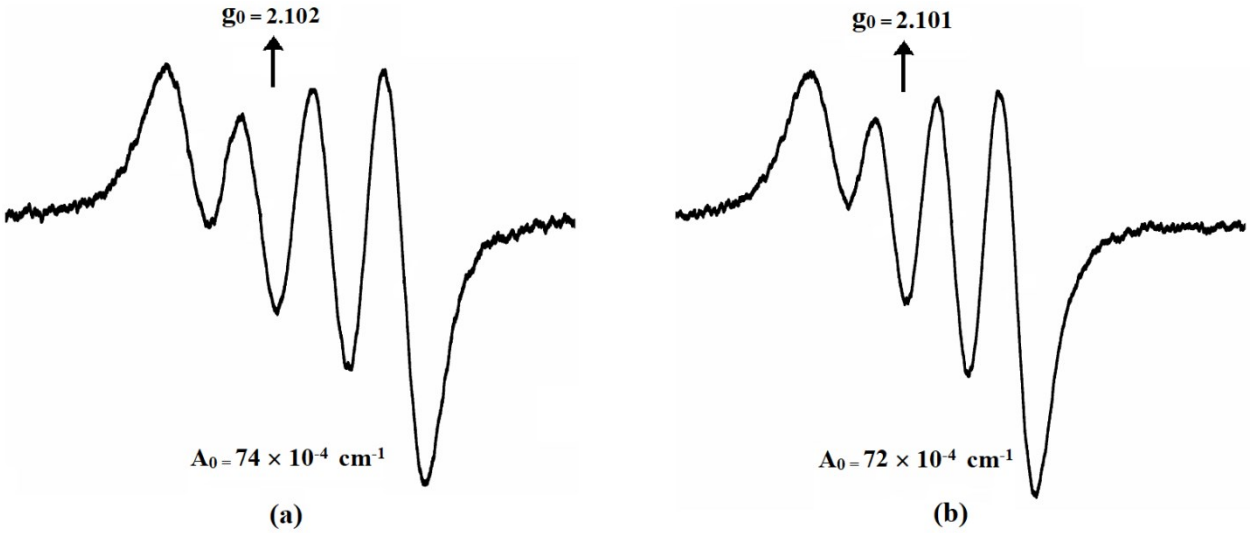

Fig. S9 Solution EPR of $[Cu(trien)(bpy)](ClO_4)_2$ **1** (a) and $[Cu(trien)(5,6\text{-dmp})](ClO_4)_2$ **3** (c) in CH_3CN : acetone (4:1 v/v) at RT.

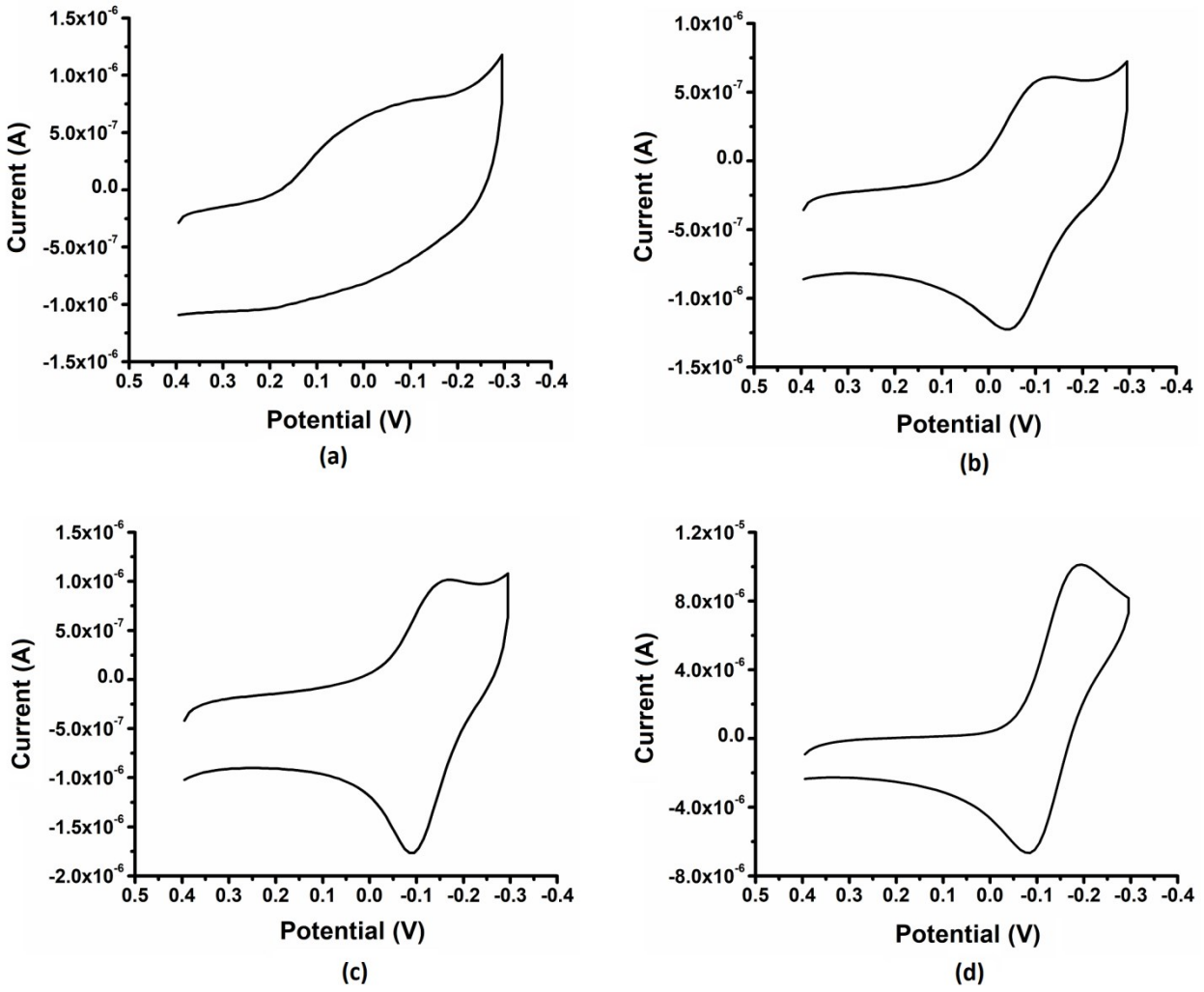

Fig. S10 Cyclic Voltammograms of $[Cu(trien)(bpy)](ClO_4)_2$ **1** (a), $[Cu(trien)(phen)](ClO_4)_2$ **2** (b), $[Cu(trien)(5,6\text{-dmp})](ClO_4)_2$ **3** (c) and $[Cu(trien)(3,4,7,8\text{-tmp})](ClO_4)_2$ **4** (d) in CH_3CN at 25 °C at 50 mVs^{-1}. Working electrode: Glassy carbon, Reference electrode: Ag/AgCl

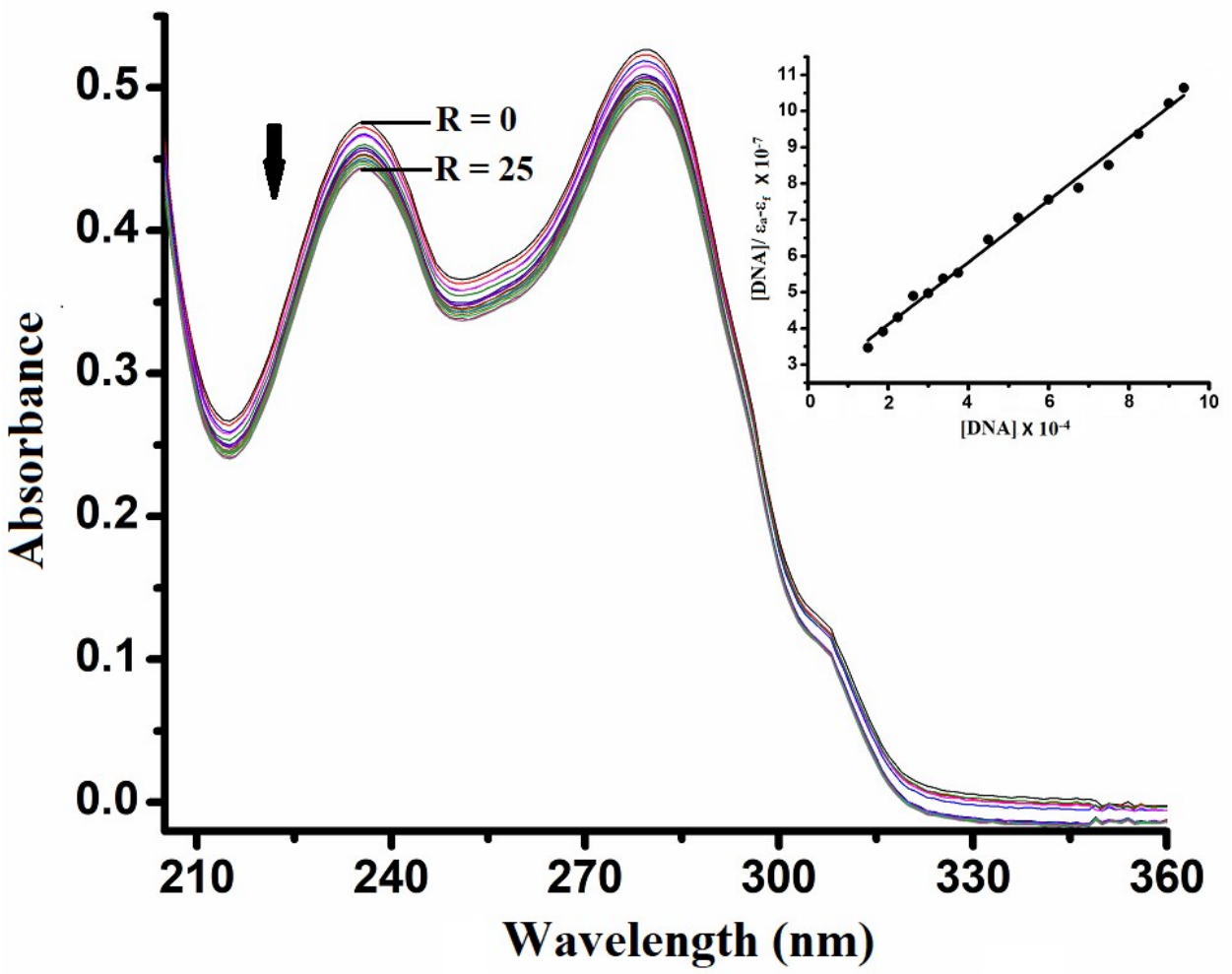

Fig.S11 Absorption spectra of [Cu(trien)(bpy)]$(ClO_4)_2$ **1** in 5 mMTris-HCl buffer at pH 7.2, in the absence (R = 0) and presence (R = 1 - 25) of increasing amounts of CT DNA. Inset: The plot of [DNA] vs. [DNA]/(ε_a-ε_f) at R=25 of the complex [Cu(trien)(bpy)]$(ClO_4)_2$ **1**.

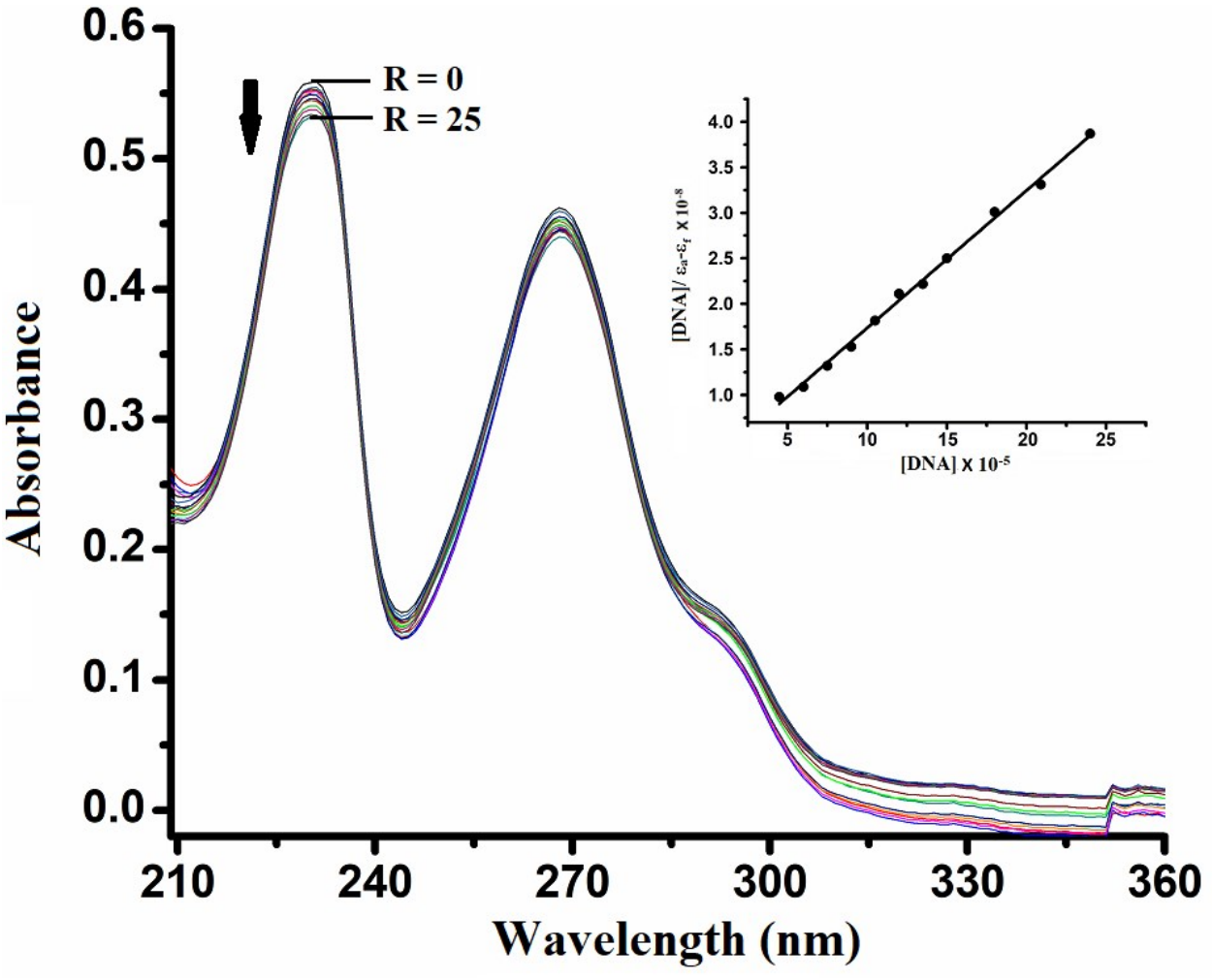

Fig. S12 Absorption spectra of [Cu(trien)(phen)]$(ClO_4)_2$ **2** in 5 mMTris-HCl buffer at pH 7.2, in the absence (R = 0) and presence (R = 1 - 25) of increasing amounts of CT DNA. Inset: The plot of [DNA] vs. [DNA]/(ε_a-ε_f) at R = 25 of the complex [Cu(trien)(phen)]$(ClO_4)_2$ **2**.

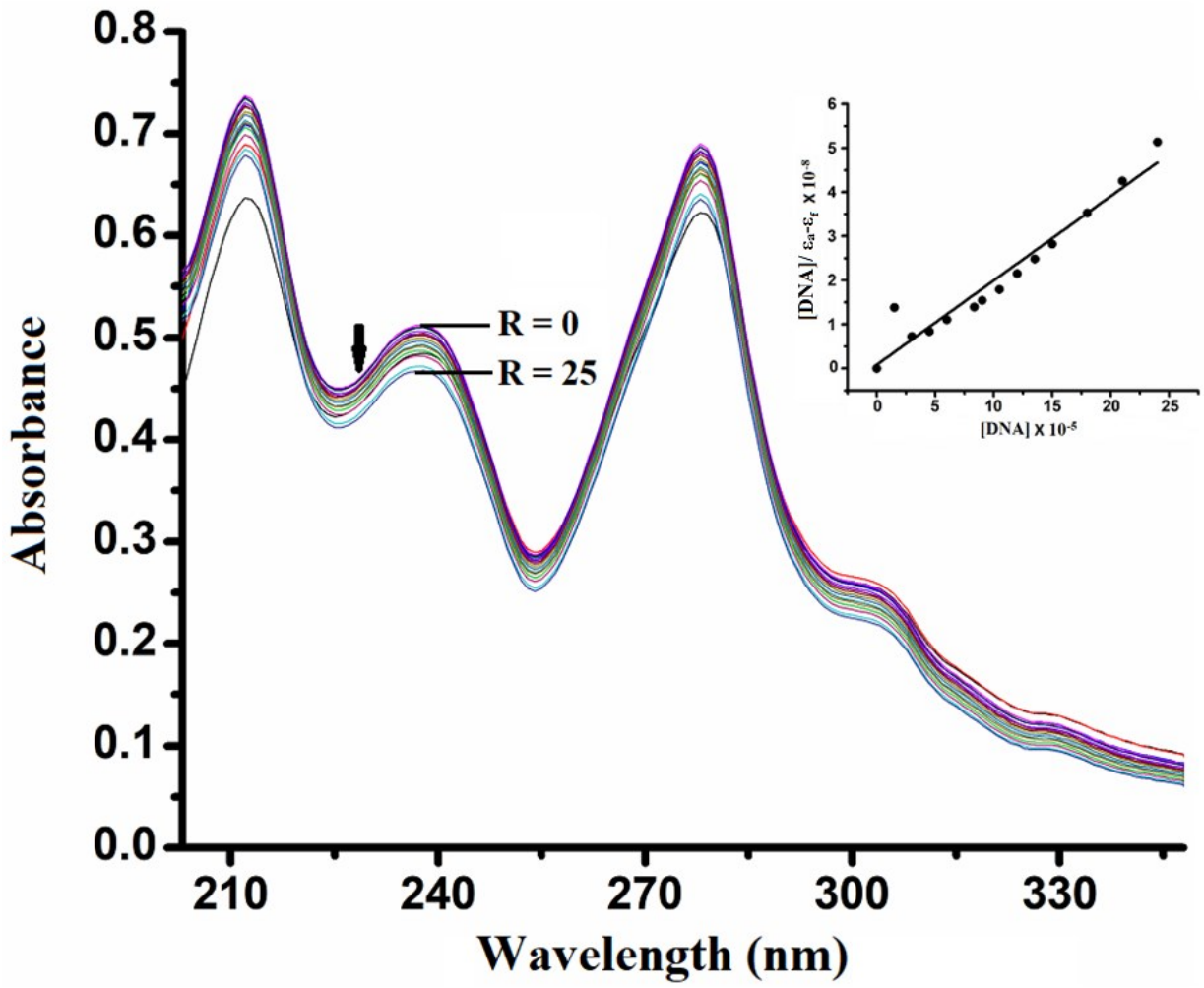

Fig. S13 Absorption spectra of [Cu(trien)(3,4,7,8-tmp)]$(ClO_4)_2$ **4** in 5 mMTris-HCl buffer at pH 7.2, in the absence (R = 0) and presence (R = 1 - 25) of increasing amounts of CT DNA. Inset: The plot of [DNA] vs. [DNA]/(ε_a-ε_f) at R=25 of the complex [Cu(trien)(3,4,7,8-tmp)]$(ClO_4)_2$ **4**.

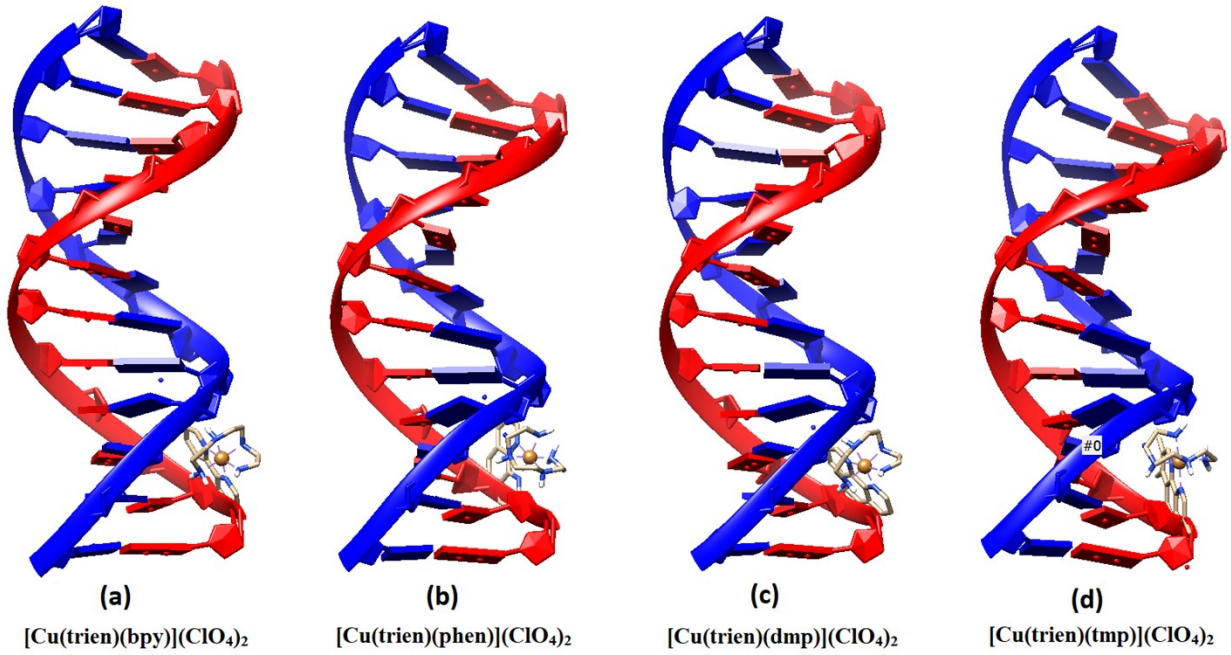

Fig. S14 Docked structures of [Cu(trien)(bpy)]$(ClO_4)_2$ **1** (a), [Cu(trien)(phen)]$(ClO_4)_2$ **2** (b), [Cu(trien)(5,6-dmp)]$(ClO_4)_2$ **3** (c) and [Cu(trien)(3,4,7,8-tmp)]$(ClO_4)_2$ **4** (d).

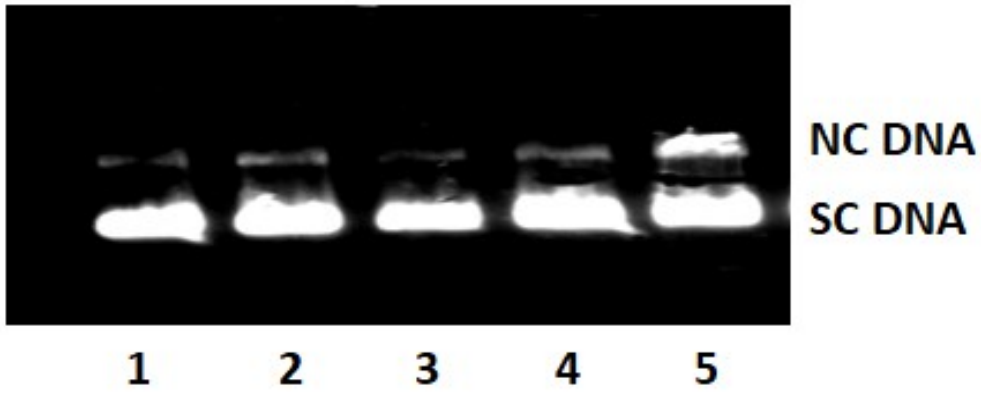

Fig. S15 Cleavage of supercoiled pUC19 DNA (40 μM) by copper(II) complexes **1** - **4** (200 μM) in absence of an external agent in Tris HCl buffer at 37 °C. Lane 1, DNA; Lane 2, DNA + **1**; Lane 3, DNA + **2**; Lane 4, DNA + **3**; Lane 5, DNA + **4**. Forms SC and NC are Supercoiled and Nicked Circular DNA respectively.

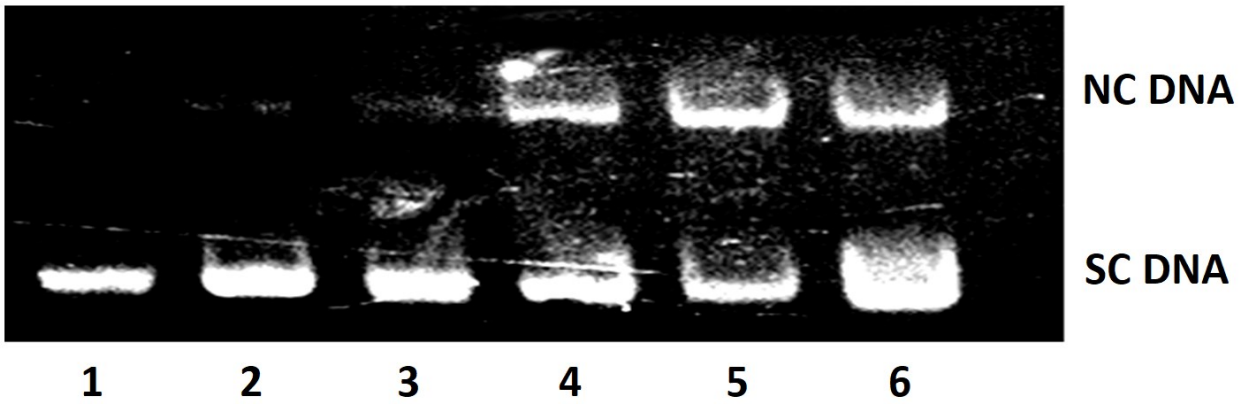

Fig. S16 Cleavage of supercoiled pUC19 DNA (40 μM) using various concentrations of $[Cu(trien)(3,4,7,8\text{-tmp})]^{2+}$ **4** for 1 h in Tris HCl buffer at pH 7.2 and 37 °C. Lane 1, DNA; Lane 2, DNA + **4** (50 μM); Lane 3, DNA + **4** (100 μM); Lane 4, DNA + **4** (300 μM); Lane 5, DNA + **4** (400 μM); Lane 6, DNA + **4** (500 μM). Forms SC and NC are Supercoiled and Nicked Circular DNA respectively.

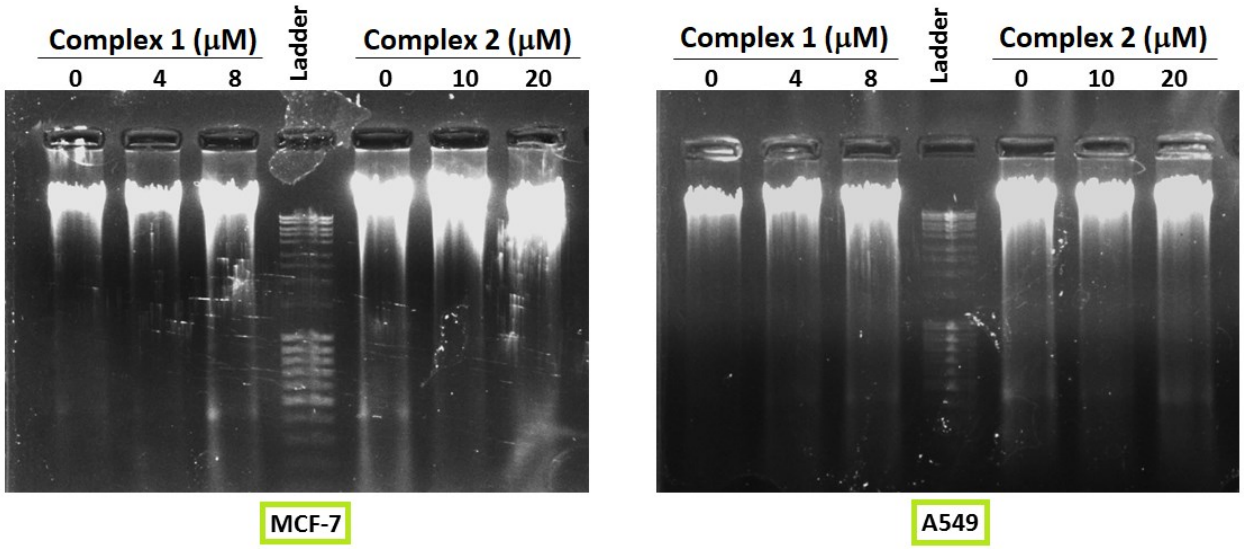

Fig. S17 DNA fragmentation assay for detection of apoptosis by treating complex Cu(trien)(bpy)]$(ClO_4)_2$ **1** (0, 4 and 8 μM) and [Cu(trien)(phen)]$(ClO_4)_2$ **2** (0, 10 and 20 μM) with MCF-7 and A549 cancer cells for 48 h.

Table S1 Electronic and EPR spectral data (λ_{max} in nm, Ɛ in M^{-1} cm^{-1}) for [Cu(trien)(diimine)]$(ClO_4)_2$ **(1-4)** in CH_3CN solution.[a]

Complex	λ_{max} in nm (ε, $M^{-1}cm^{-1}$)	Assignment	EPR[d]
1	574 (160) 277 (46400) 242 (37000) 237 (38000)	[b]LF [c]Ligand-based [c]Ligand-based	$g_{\|}$=2.204 $g_{\perp}$= 2.045 $A_{\|}$=188× 10^{-4} cm^{-1}
2	582 (210) 265 (41330) 227 (32200) 202 (24400)	[b]LF [c]Ligand-based [c]Ligand-based	$g_{\|}$=2.203 $g_{\perp}$= 2.046 $A_{\|}$=186× 10^{-4} cm^{-1}
3	591 (152) 269 (35730) 233 (44800) 203 (17730)	[b]LF [c]Ligand-based [c]Ligand-based [c]Ligand-based	$g_{\|}$=2.205 $g_{\perp}$= 2.058 $A_{\|}$=189× 10^{-4} cm^{-1}
4	648 (102) 275 (46330) 239 (36070) 211 (45600)	[b]LF [c]Ligand-based [c]Ligand-based [c]Ligand-based	$g_{\|}$=2.206 $g_{\perp}$= 2.061 $A_{\|}$=173× 10^{-4} cm^{-1}

[a]Concentration, 0.015 mM - 5mM; [b]LF, Ligand Field; [c]LMCTand Ligand-based transitions; [d]Frozen solution EPR in CH_3CN : acetone (4:1 v/v) at LNT.

Table S2 Electrochemical data of Cu(II) Complexes, [Cu(trien)(diimine)]$(ClO_4)_2$ **(1-4)**.

Complex	E_{pc} **(V)**	E_{pa} **(V)**	ΔE_p **(mV)**	$E_{1/2}$ **(V)**
[Cu(trien)(bpy)]$(ClO_4)_2$ **1**	-0.097 0.051	- 0.195	- 144	0.100[a] 0.123[b]
[Cu(trien)(phen)]$(ClO_4)_2$ **2**	-0.129	-0.040	89	-0.085
[Cu(trien)(dmp)]$(ClO_4)_2$ **3**	-0.168	-0.090	78	-0.129
[Cu(trien)(tmp)]$(ClO_4)_2$ **4**	-0.195	-0.082	113	-0.139

Measured *vs.* non-aqueous Ag/Ag^+ reference electrode; Supporting electrolyte, TBAB (0.1 M); Complex concentration, 1 mM; Cyclic Voltammetry, scan rate 50 mVs^{-1}, [a]$E_{pc1/2}$, potential at half height. [b]scan rate 25 mV s^{-1}

Table S3 Cleavage data of SC pUC19 DNA (40 μM) by complexes **1**-**4** (200 μM) in the absence of an external agent in a Tris HCl buffer at 37 °C.

Lane number	Reaction conditions	Form (%)	
		SC	NC
1	DNA	95.1	4.9
2	DNA + **1** (200 μM)	83.3	16.7
3	DNA + **2** (200 μM)	84.9	15.1
4	DNA + **3** (200 μM)	80.5	19.5
5	DNA + **4** (200 μM)	70.8	29.2

Table S4 Concentration-dependent cleavage data of SC pUC19 DNA (40 μM) by complex **4** in the absence of an external agent in a buffer containing 5 mM TrisHCl/50 mM NaCl at 37 °C.

Lane number	Reaction conditions	Form (%)	
		SC	NC
1	DNA	97.9	2.1
2	DNA + **4** (50 μM)	91.8	8.2
3	DNA + **4** (100 μM)	80.7	19.3
4	DNA + **4** (300 μM)	54.6	45.4
5	DNA + **4** (400 μM)	42.8	57.2
6	DNA + **4** (500 μM)	41.2	58.8

Table S5 IC_{50} values of trien and diimine ligands, $Cu(ClO_4)_2 \cdot 6H_2O$ and dien and trien (**1-4**) complexes against MCF-7 and A549 cancer cell lines in three independent experiments.

Compounds	**MCF-7 (µM)**					**A549 (µM)**				
	SET1	SET2	SET3	Avg	Graph Pad	SET1	SET2	SET3	Avg	Graph Pad
trien	10.5	1.0	11.2	7.6 ± 0.6	5.2	13.0	9.1	16.2	12.8 ± 0.4	12.6
Cu	5.4	4.3	9.4	6.4 ± 0.3	6.1	9.8	16.8	22.1	16.3 ± 0.6	19.2
$[Cu(dien)(bpy)]^{2+}$	12.8	9.3	16.0	12.7 ± 0.3	12.8	9.2	19.8	20.8	16.7 ± 0.6	20.4
$[Cu(dien)(phen)]^{2+}$	4.1	3.6	4.8	4.2 ± 0.5	4.2	4.2	4.1	3.8	4.1 ± 0.2	4.0
bpy	4.8	3.5	5.6	4.7 ± 0.5	4.5	5.1	5.6	5.0	5.3 ± 0.3	5.3
phen	11.0	2.1	5.0	6.1 ± 0.5	5.0	7.0	11.5	2.5	7.1 ± 0.5	6.5
5,6-dmp	6.4	4.8	6.3	5.9 ± 0.9	5.9	5.2	6.0	6.3	5.9 ± 0.6	6.2
3,4,7,8-tmp	6.9	4.6	7.4	6.4 ± 0.2	6.3	3.9	4.7	5.1	4.6 ± 0.9	4.7
1	3.2	4.0	4.6	3.9±0.6	3.7	3.2	3.1	3.6	3.3±0.2	3.2
2	13.3	9.7	10.9	11.3±0.2	10.6	8.9	10.3	12.3	10.5±0.2	9.8
3	0.9	2.9	2.8	2.1±0.9	2.0	28.0	21.5	27.3	25.6±0.3	23.5
4	>50	>50	>50	>50	>50	18.1	17.5	20.8	18.8±0.2	17.2